

Supporting Information for

**Concentrations and Properties of Ice Nucleating Substances from Exudates of Antarctic Sea-Ice
Diatoms**

Yu Xi^a, Alexia Mercier^b, Cheng Kuang^c, Jingwei Yun^a, Ashton Christy^a, Luke Melo^a, Maria T. Maldonado^c,
James A. Raymond^d, Allan K. Bertram^a

^aDepartment of Chemistry, University of British Columbia, 2036 Main Mall, Vancouver, BC V6T 1Z1, Canada.

^b Department of Chemistry, Sorbonne University, 21 rue de l'École de médecine 75006 Paris, France.

^c Department of Earth, Ocean & Atmospheric Sciences, University of British Columbia, 2020 – 2207 Main Mall, Vancouver, BC
V6T 1Z4, Canada.

^d School of Life Sciences, University of Nevada, 4505 S. Maryland Pkwy., Las Vegas, NV89154, USA.

Contents of this file

Text S1

Figures S1 to S5

Text S1.

We employ a machine vision algorithm written in MATLAB to determine the freezing point of each droplet in the droplet freezing experiments. In these experiments, a camera records a video while the temperature is decreased at a rate of 3°C/min. In the video, liquid droplets appear as dark-colored spots which turn bright upon freezing, while the background remains a constant gray tone. Our algorithm locates the spots using the final frame in the video. We crop the frame to isolate the location of the three hydrophobic glass slides within the field of view, then binarize the cropped frame. We choose a binarization threshold by dividing the cropped frame into 64 regions, and computing mean pixel intensities for each region. Any pixels in the 64 regions that exceed the local mean are set equal to 1, while those that fall below it are set equal to 0. This isolates any bright spots within the frames (see Fig. S5a), while accounting for local variations in intensity due to inhomogeneity¹. We then calculate various geometric properties of these spots, and select those which are most likely to be droplets: we exclude spots occupying less than 0.016% or greater than 0.14% of the cropped video frame, as well as those whose eccentricity exceeds 0.8, and those whose solidity (the ratio of the spot's area to that of the convex hull containing it) is less than 0.85. Figure S5b shows the results of this geometric detection overlaid on the cropped frame, with detected spots circled in red. Notably, the detected spots on the top-right of the frame only cover part of the droplets; this is due to inhomogeneous lighting in the sample mount.

We then track the brightness of each spot by extracting the pixel brightness at each spot's centroid through each video frame. Figure S5c shows each spot's centroid, labeled and indexed, and Figure S6a shows an example of the brightness of each spot's centroid during a typical freezing experiment. From the time dependence of the brightness of each spot's centroid, we then calculate the first derivative of the brightness of each spot's centroid as a function of the frame number (see Fig. S6b as an example). The freezing point was then assigned to the frame where the first derivative of the brightness reaches a maximum. During the freezing experiments, the temperature was also recorded as a function of time. As the video camera collects frames at a faster rate than the temperature is recorded, we apply a piecewise polynomial spline to interpolate temperature data to correspond with each video frame. We then determine the freezing time and temperature for each droplet by attributing a timestamp to the selected frame, and finding the temperature at that time point.

After determining the freezing temperature of each droplet, we then assigned each droplet to one of three clusters, representing the three hydrophobic glass slides used in the freezing experiments. This was done by applying k-means clustering to the detected spot centroids. The k-means clustering optimizes a partition in a dataset by minimizing the distance between the mean of a cluster and each data point^{2,3}. Once the spots have been partitioned into clusters, we determine the time and temperature at which 50% of the droplets have frozen (T_{50}) for each hydrophobic glass slide, as well as a list of droplet freezing temperatures corresponding to each hydrophobic glass slide.

To test the accuracy of the machine vision algorithm, we conducted a comparison of the freezing temperatures determined with the MATLAB script with those produced by manual analysis. Out of 660 droplets analyzed, we found the MATLAB script correctly identified the freezing temperature of 98.5% of the droplets, to within 0.2 °C, which is less than the uncertainty of the measurements. 1.5% of the droplets had different values between manual and MATLAB results (i.e., outside the 0.2 °C tolerance); these were generally due to the MATLAB script incorrectly identifying the freezing point. In all cases, the MATLAB script correctly identified the T_{50} values of the droplets to within 0.1 °C, for each hydrophobic glass slide analyzed.

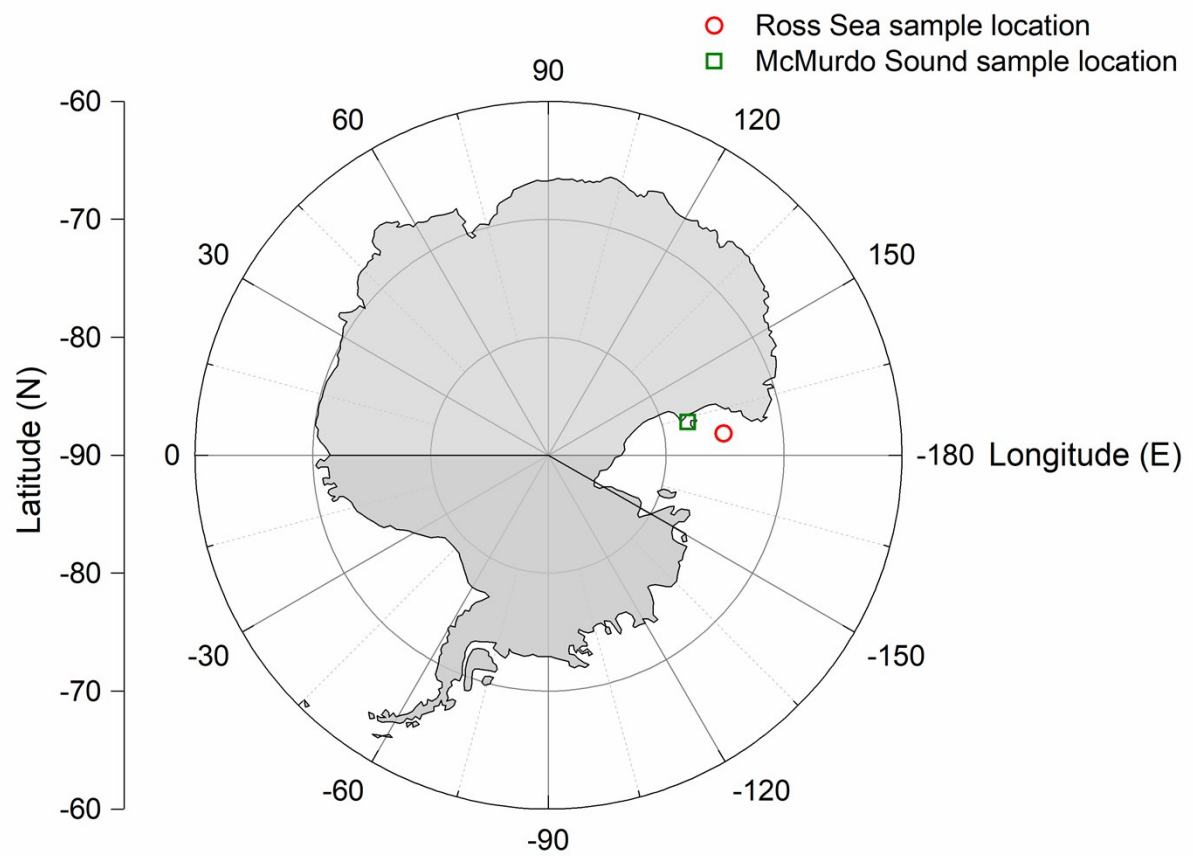


Figure S1. Map showing the locations at which the samples were collected.

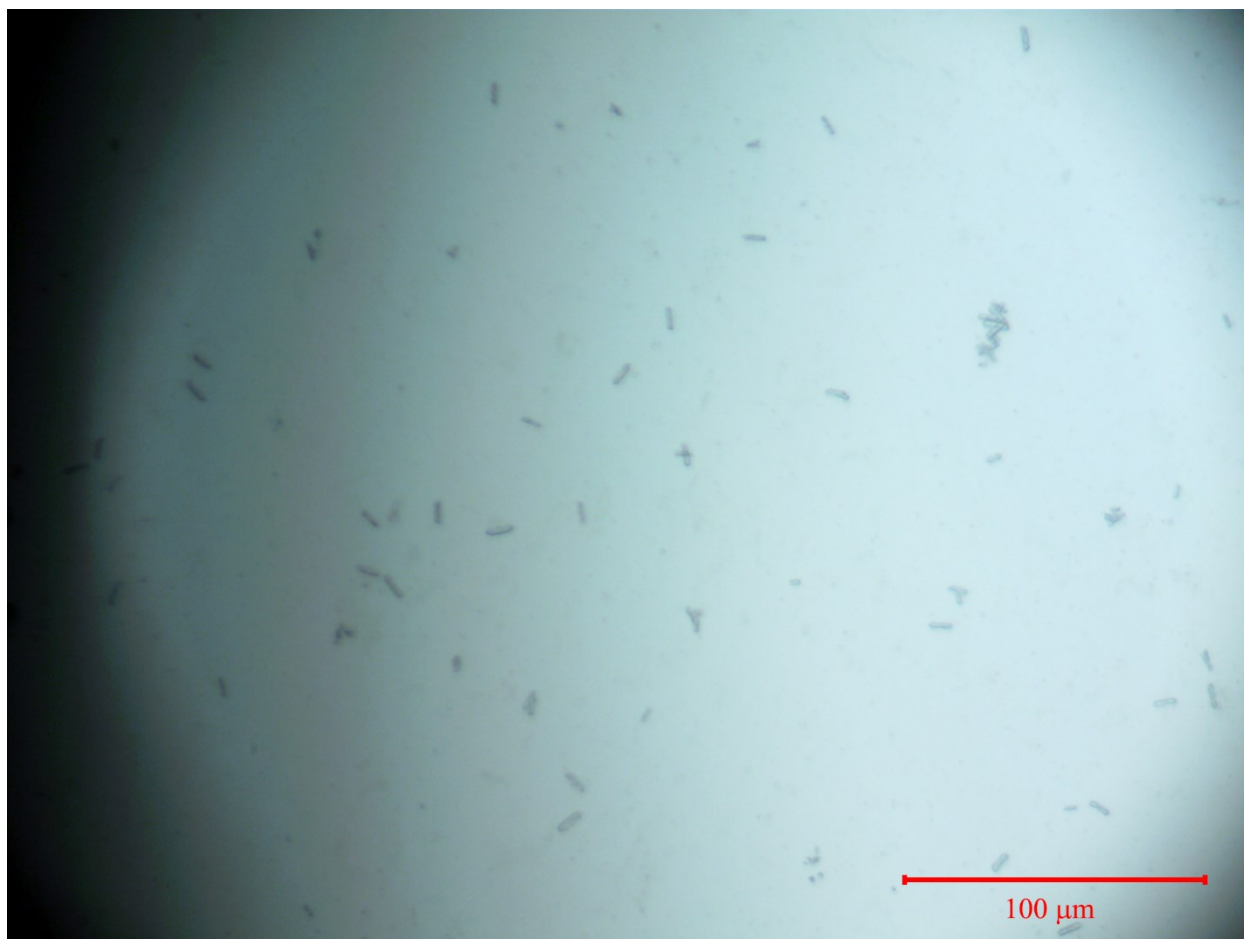


Figure S2. Images of diatom cells from the freeze-dried sample collected at McMurdo Sound. Images were taken with an optical microscope (20× objective). To generate a slide for imaging, a 5 wt % suspension of the freeze-dried sample in MilliQ water was prepared, and then a 1 μL droplet of the suspension was pipetted on a plain glass microscope slide and covered with a cover slide.

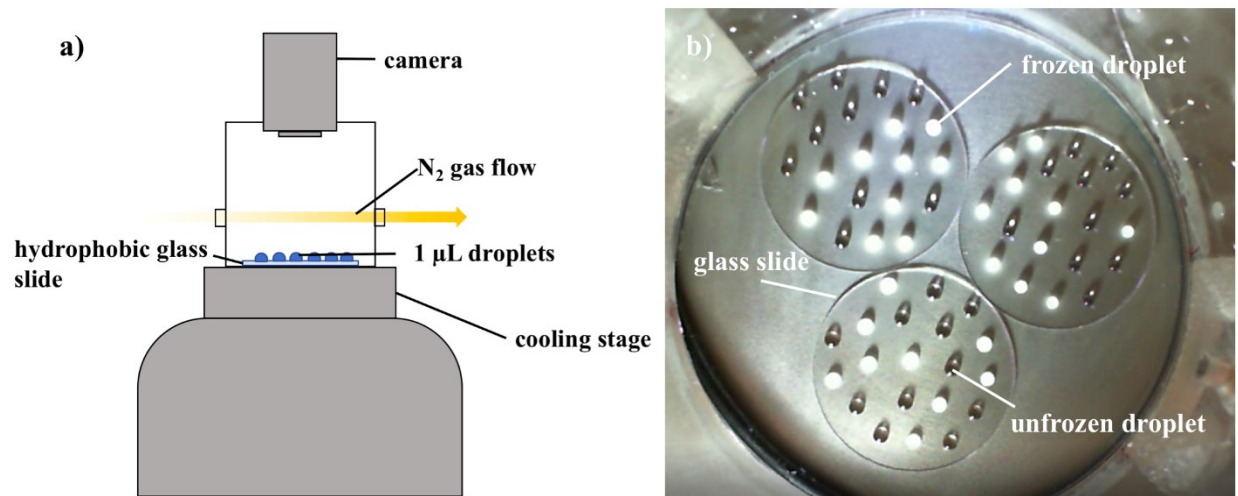


Figure S3. a) Illustration of the setup for droplet freezing experiments; b) image of droplets taken at around -25 °C during a freezing experiment. The diameter of the glass slides in panel b is 18 mm.

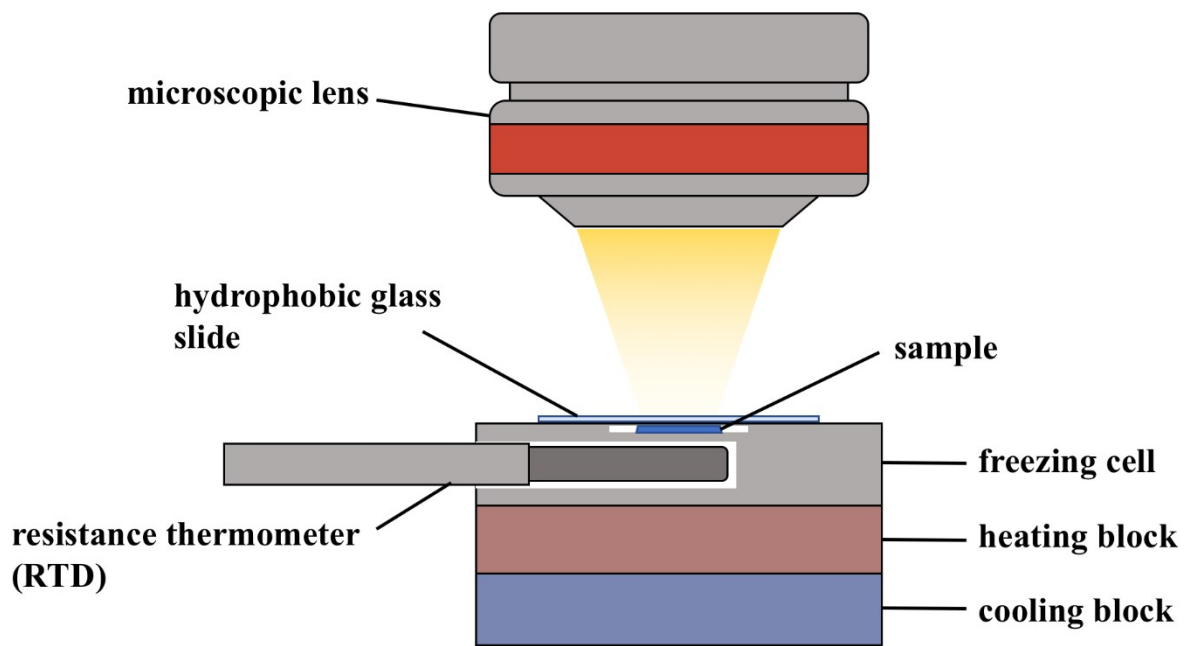


Figure S4. Illustration of the experimental setup for melting point measurements.

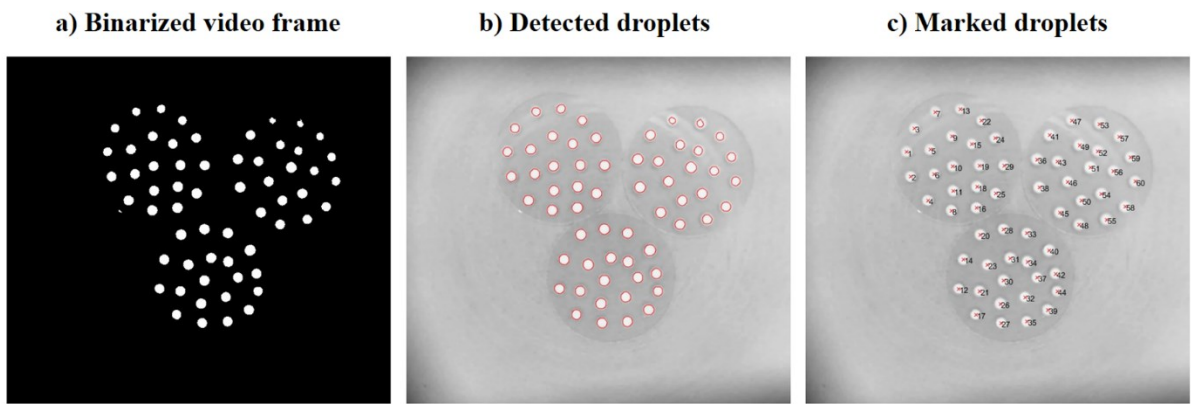


Figure S5 Graphs showing a) binarized video frame, b) detected droplets, and c) detected droplets with centroids marked and indexed ($n = 1-60$).

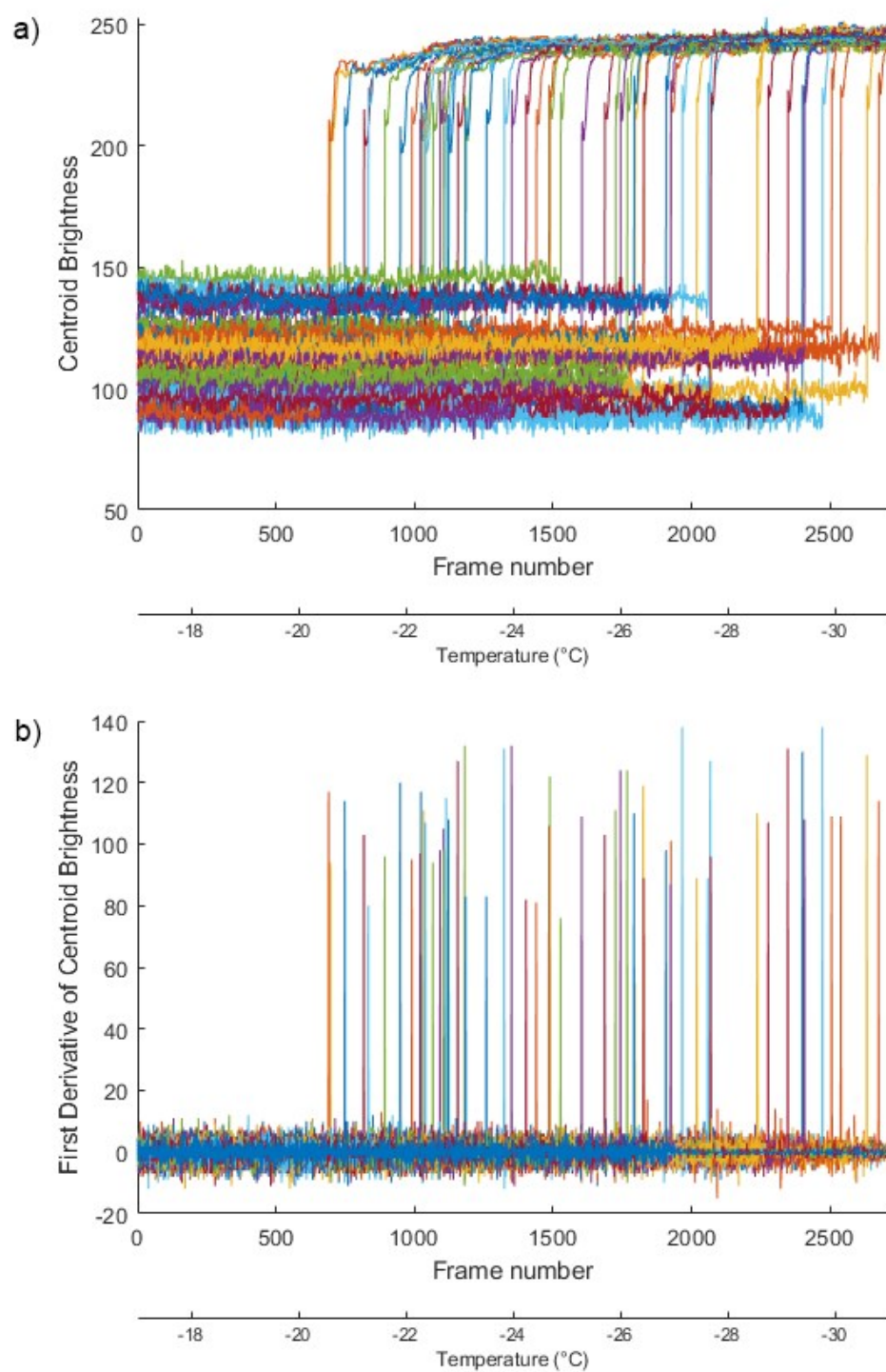


Figure S6 a) Centroid brightnesses and b) first derivative of centroid brightnesses during a freezing experiment.

Bibliography

- 1 D. Bradley and G. Roth, Adaptive Thresholding using the Integral Image, *J. Graph. Tools*, 2007, **12**, 13–21.
- 2 A. K. Jain, Data clustering: 50 years beyond K-means, *Pattern Recognit. Lett.*, 2010, **31**, 651–666.
- 3 H. Steinhaus, On the Division of Material Bodies into Parts, *Bull. Acad. Pol. Sci.*, 1956, 801.